Quarterly Technical Report No. 2

Covering the Period 31 January 1972 - 30 April 1972

DEVELOPMENT OF GaAs SOLAR CELLS

Contract No. 953270

Jet Propulsion Laboratory
California Institute of Technology
4800 Oak Grove Drive
Pasadena, California 91103

Approved by: F. T. C. Bartels
Division Manager

Philip J. McNally
Principal Investigator

May 1972

ION PHYSICS CORPORATION IPC

A Subsidiary of High Voltage Engineering Corporation

BURLINGTON, MASSACHUSETTS

This report contains information prepared by Ion Physics Corporation under JPL Subcontract. Its content is not necessarily endorsed by the Jet Propulsion Laboratory, California Institute of Technology, or the National Aeronautics and Space Administration.

Quarterly Technical Report No. 2

Covering the Period 31 January 1972 - 30 April 1972

DEVELOPMENT OF GaAs SOLAR CELLS

Contract No. 953270

Jet Propulsion Laboratory
California Institute of Technology
4800 Oak Grove Drive
Pasadena, California 91103

Approved by:

F. T. C. Bartels
Division Manager

Philip J. McNally
Principal Investigator

This work was performed for the Jet Propulsion Laboratory, California Institute of Technology, sponsored by the National Aeronautics and Space Administration under Contract NAS7-100.

ION PHYSICS CORPORATION
BURLINGTON, MASSACHUSETTS

TABLE OF CONTENTS

LIST OF ILLUSTRATIONS

SUMMARY

During this report period the experimental phase of this program was initiated. Ion implantation of zinc in GaAs to form highly doped p-type surface layers and electrical characterization of these layers was performed. Annealing characteristics of implant energies between 200 keV and 1.4 MeV and zinc dose levels between 5×10^{14} cm^{-2} and 5×10^{15} cm^{-2} were investigated. Junction depth measurements as a function of implant energy were made. The preliminary results show that additional effort should be expended in the energy region of 600 - 800 keV and zinc dose levels between 10^{15} and 5×10^{15} cm^{-2} to optimize the implant parameters for cell fabrication. Surface preparation, contact metallurgy and junction characteristics are also discussed.

SECTION 1

INTRODUCTION

This is the second quarterly technical report on a program, the goal of which is to achieve high efficiency GaAs solar cells. The program has been divided into three phases which were discussed in detail in the first quarterly report. Phase I - analytical was concerned with providing design information for use in experimentally determining optimum solar cell process parameters. The first quarterly report contained the results of those design calculations. Using those results as a guide, work was initiated on Phase I - experimental to determine optimum cell process parameters. The initial results on this phase of the program is the subject of this report.

SECTION 2

EXPERIMENTAL INVESTIGATIONS

2.1 Introduction

The experimental phase of this program has as its objective the determination of optimum implantation and device process parameters necessary to achieve high efficiency GaAs solar cells. To accomplish this objective the cell has been divided into four areas of experimental investigation which focus on one or more important cell characteristics. These experimental areas are:

(1) Surface Preparation and Protection

- Surface recombination velocity

(2) Surface Layer Characterization

- Doping concentration - sheet resistance
- Minority carrier lifetime and diffusion length
- Doping concentration profile - drift field
- Junction depth - x_j/L ratio

(3) Junction Characteristics

- Space charge generation - recombination

(4) Electrical Contacts and Antireflection Coating

- Series Resistance
- Quantum Efficiency

The analytical results discussed in Quarterly Report No. 1 are being used to guide the selection of experimental conditions in these investigations. The results in that report showed the P/N cell polarity to have the higher calculated cell efficiency. Therefore implantation of zinc ions to form p-type surface layers was selected for initial study. The analytical results also showed that near optimum cell design consists of a surface layer concentration, N_S = 2×10^{19} cm^{-3}, substrate concentration, $N_B = 2 \times 10^{17}$ cm^{-3}, junction depth, $x_j = 0.5$ μm, and corresponding sheet resistance of ~ 100 $\Omega/\square$. The experimental work is directed toward achieving these results and was concentrated in the areas of surface preparation and protection and surface layer characterization during this report period. Preliminary work on junction characterization and electrical contacts was also started during this period.

2.2 Zinc Implantation

2.2.1 Experimental Procedures

The starting GaAs substrate material consisted of boat grown n-type wafers 20 mils thick (1-1-1) orientation with background concentrations of 1×10^{16} cm^{-3} (0.1 Ω cm) and 2×10^{17} cm^{-3} (0.009 Ω cm). After some experimenting with several polishing procedures, the technique which evolved and used on these wafers consisted of two steps. The first step consisted of chemical-mechanical polishing on a politex pad with 2% sodium hypochlorite solution to remove all surface work damage from the original sawing operation of the material supplier. This was followed by a final etch in 5% bromine-methanol solution to remove any residual work damage from the chemical-mechanical polishing step. The total thickness of material removed was 4-5 mils. This technique was found to be capable of close control over the amount of material removed and produced flat damage free surfaces. After surface preparation the wafers were given a thorough clean-up and degreasing prior to implantation.

Zinc implantations were performed with the samples misaligned 7 ° to the ion beam to minimize possible channeling effects. Implantation was performed with the substrates held at room temperature.

Post implantation annealing is required to remove radiation damage and enhance the electrical activity of the implanted ions. Isochronal annealing was performed between 400 °C and 800 °C for one-half hour intervals in a forming gas atmosphere. Annealing above 600 °C requires that the GaAs surface be protected against dissociation and possible out diffusion of the implanted ions. This protection can be accomplished by either annealing in a quartz ampoule containing an arsenic overpressure or by oxide coating of the sample surface. The latter technique was chosen for this work since it simplified the experimental work and affords protection to the surface in subsequent processing steps. The oxide coating consisted of 3000 Å of SiO_2 deposited at approximately 80 °C by a high vacuum-ion beam sputtering process. This process is used by Ion Physics to deposit integral coverslips on silicon solar cells, the details of which are described in numerous reports.[1] Samples annealed up to 800 °C show no apparent visible degradation with this coating. Annealing was performed on bare samples between 400 °C and 600 °C at 50 °C intervals for one-half hour. Following the 600 °C anneal the samples were coated with SiO_2. The oxide coated samples were scribed into several pieces to complete the remaining anneals. After each anneal the oxide was stripped from the sample and sheet resistance and junction depth measurements were made. The samples were retained for subsequent processing into diodes for junction characterization.

---

[1] See for example, Ion Physics Reports on "Solar Cell Cover Glass Development" Contract No. NAS5-10236 NASA Goddard Space Flight Center, Greenbelt, Maryland, (1968 - 1971).

2.2.2 Surface Layer Characteristics

Post implantation annealing is required to remove the radiation damage caused by the interaction of the implanted ions and the GaAs lattice and to enhance the substitution of the implanted ions onto electrically active lattice sites. The extent to which these processes are accomplished determines several important cell parameters which are dependent on surface layer and junction properties. In particular sheet resistance, minority carrier transport and junction behavior are affected by the annealing process.

Figure 1 contains the results of sheet resistance versus annealing temperature for 600 keV and 800 keV and 10^{15} cm^{-2} dose in 1 x 10^{16} cm^{-3} background concentration material. After implantation a high value of sheet resistance is observed up to anneal temperatures where a significant fraction of radiation damage is annealed and the implanted ions begin to dominate the conductivity of the layer. Thermal probe readings indicated conversion to p-type conductivity occurred in the 550 ° - 600 °C temperature interval for these samples. Sheet resistance continues to decrease at progressively higher temperatures until a limiting value is reached representing a maximum in the carrier concentration-mobility product of the layer. Using the values for resistivity and mobility for bulk GaAs of Sze and Irvin[2] and measured junction depth given in Table 1, the 600 and 800 keV implants produce average carrier mobility of ~80 and 70 cm^2 V^{-1} sec^{-1} respectively.

Figures 2 through 8 show similar data for zinc implants in n-type material with N_B = 2 x 10^{17} cm^{-3} for a larger range of implant energies and fluences. The annealing behavior of these samples differed from those above in that immediately after implantation all samples exhibited low resistivity corresponding to the substrate resistivity (.009 Ω cm). The samples showed high resistance values following the 400 °C anneal similar to those above for the range of implant energies and fluences used. This is the temperature region where radiation damage begins to anneal. The temperature interval between ~450 °C and ~550 °C showed wide variation in annealing behavior which appears to be implant energy, dose and substrate dependent. At progressively higher implant energies significant coupling between the surface region and substrate occurs where electrically the surface region is in parallel with the low resistivity substrate. Another factor influencing the measurements in this region is the fact that the surface layer can remain n-type after nearly all damage is annealed. This condition can remain until the minimum electrical activity of the implanted ions exceeds the substrate carrier concentration. This occurs in the temperature interval of 550 °C - 600 °C where thermal probing also shows conversion to p-type conductivity for these samples. The anneal behavior above 600 ° C is similar to that observed in the lower concentration substrate samples. This is the temperature region of primary interest to the work on this program.

---

[2] Sze, S. M. and Irvin, J. S., Solid State Electronics II, 599 - 602 (1968).

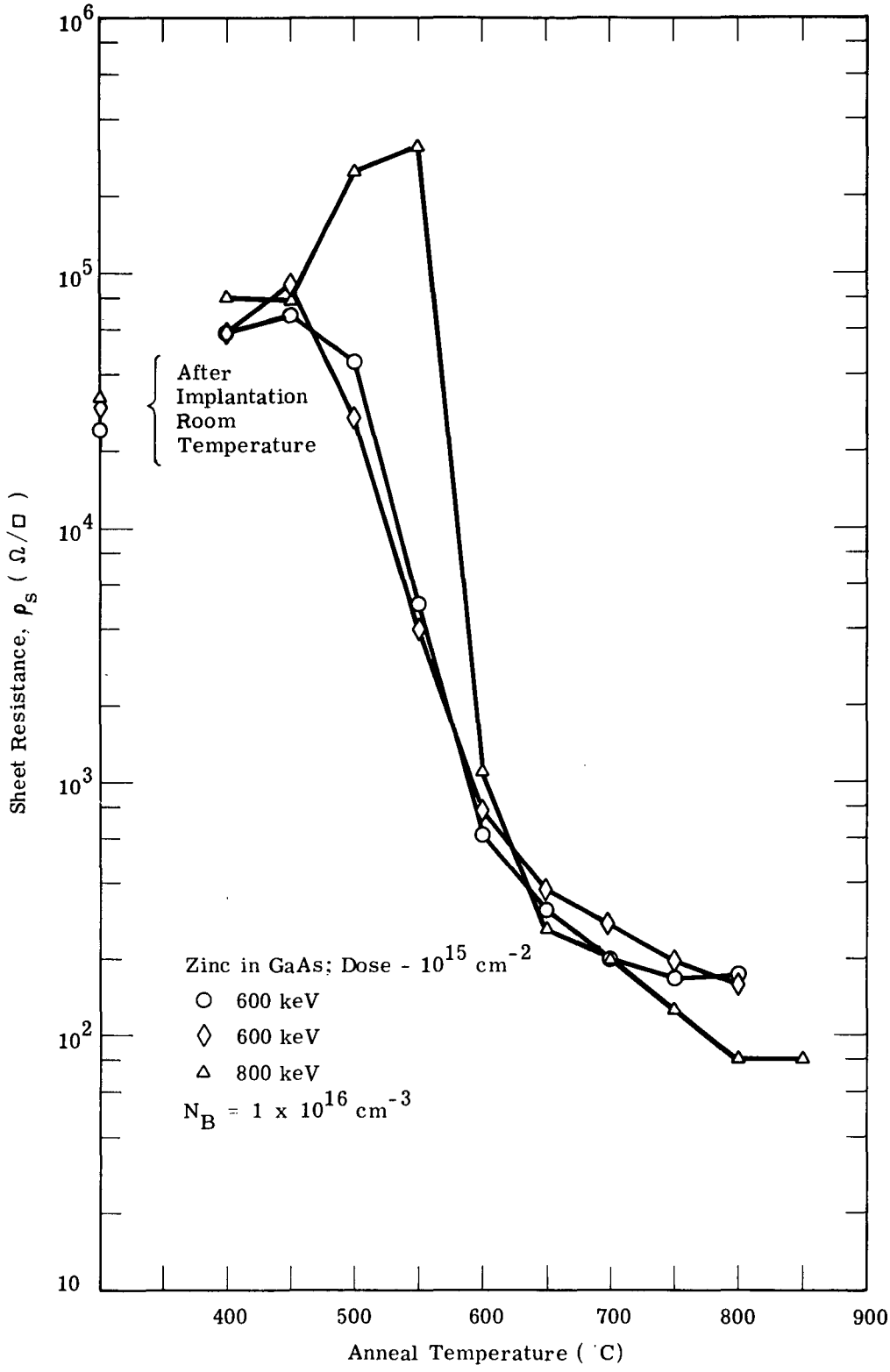

Figure 1. Sheet Resistance versus Annealing Temperature for 600 and 800 keV Zinc in GaAs and 10^{15} cm^{-2} Dose.

1-6360

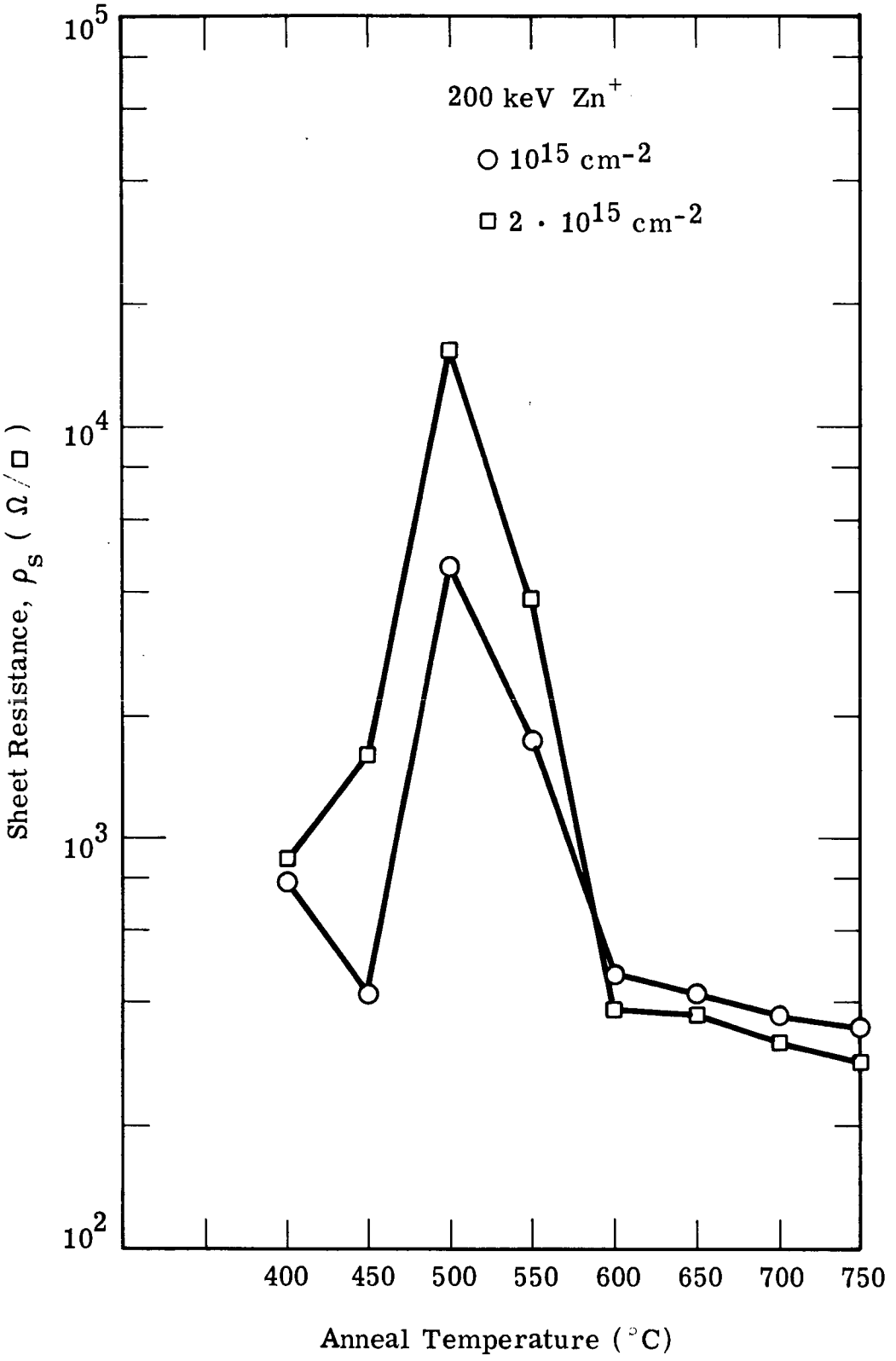

Figure 2. Annealing Characteristics for 200 keV Zinc Implants in GaAs.

1-6361

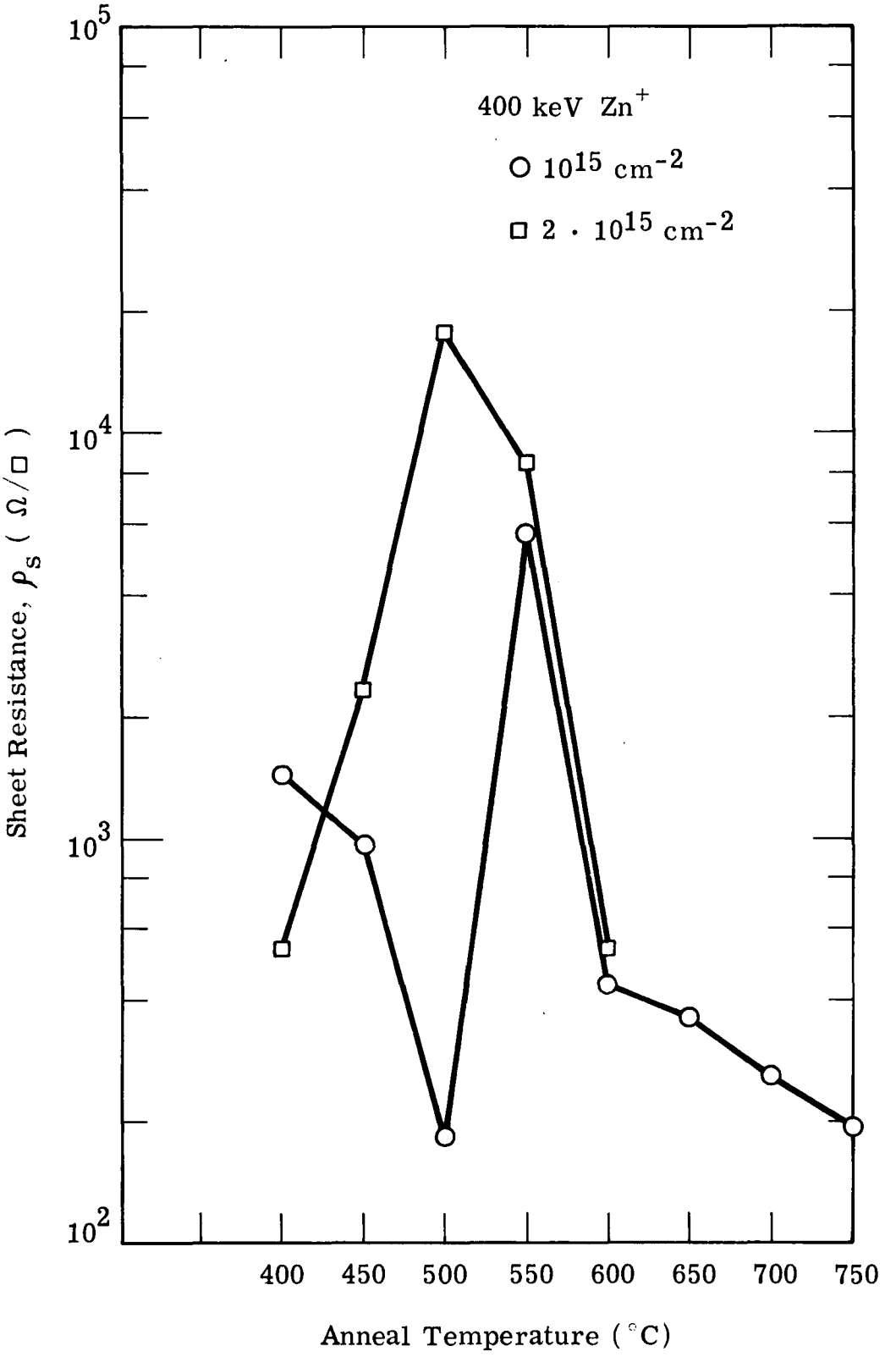

Figure 3. Annealing Characteristics for 400 keV Zinc Implants in GaAs.

1-6362

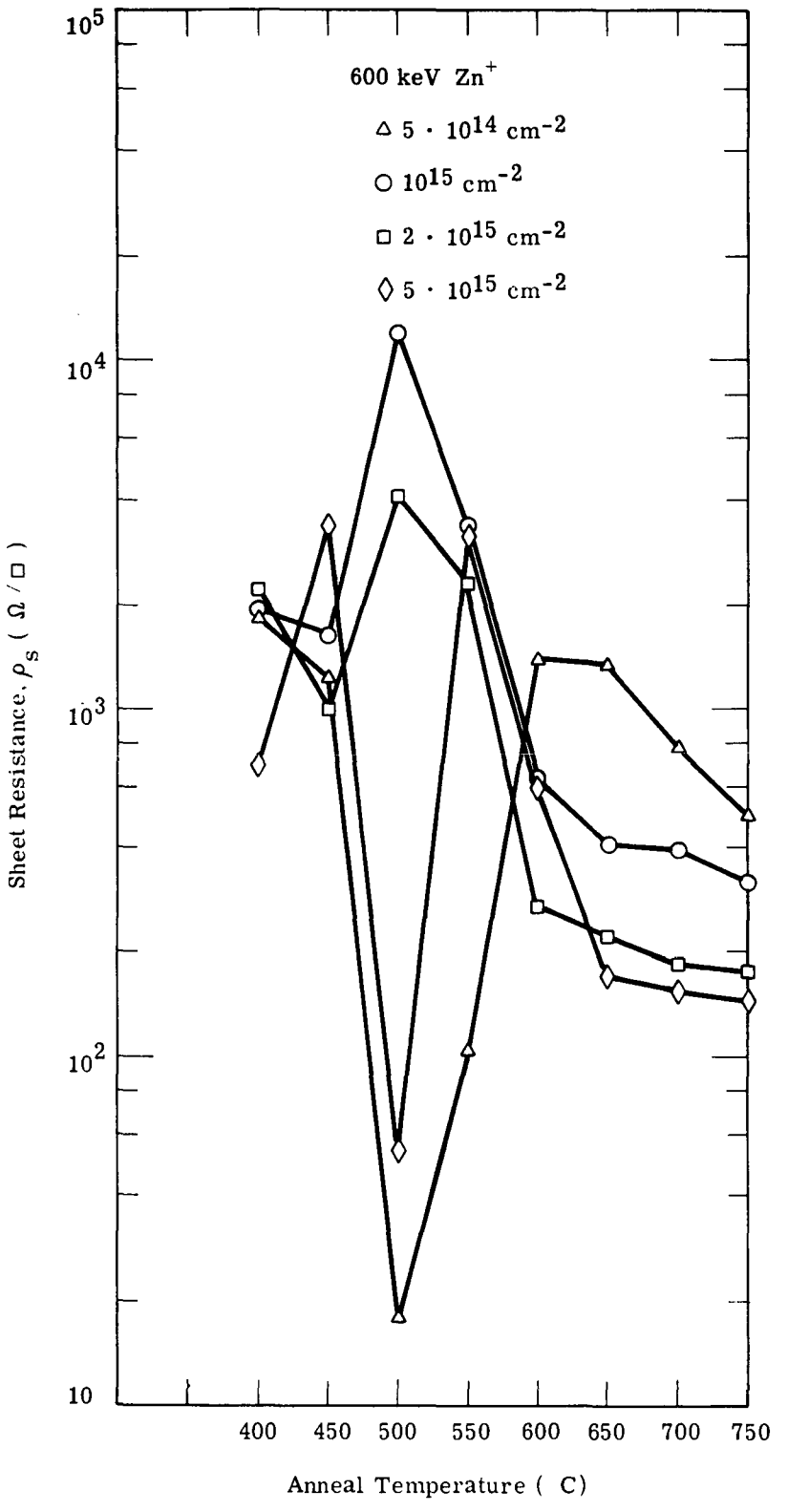

Figure 4. Annealing Characteristics for 600 keV Zinc Implants in GaAs.

1-6363

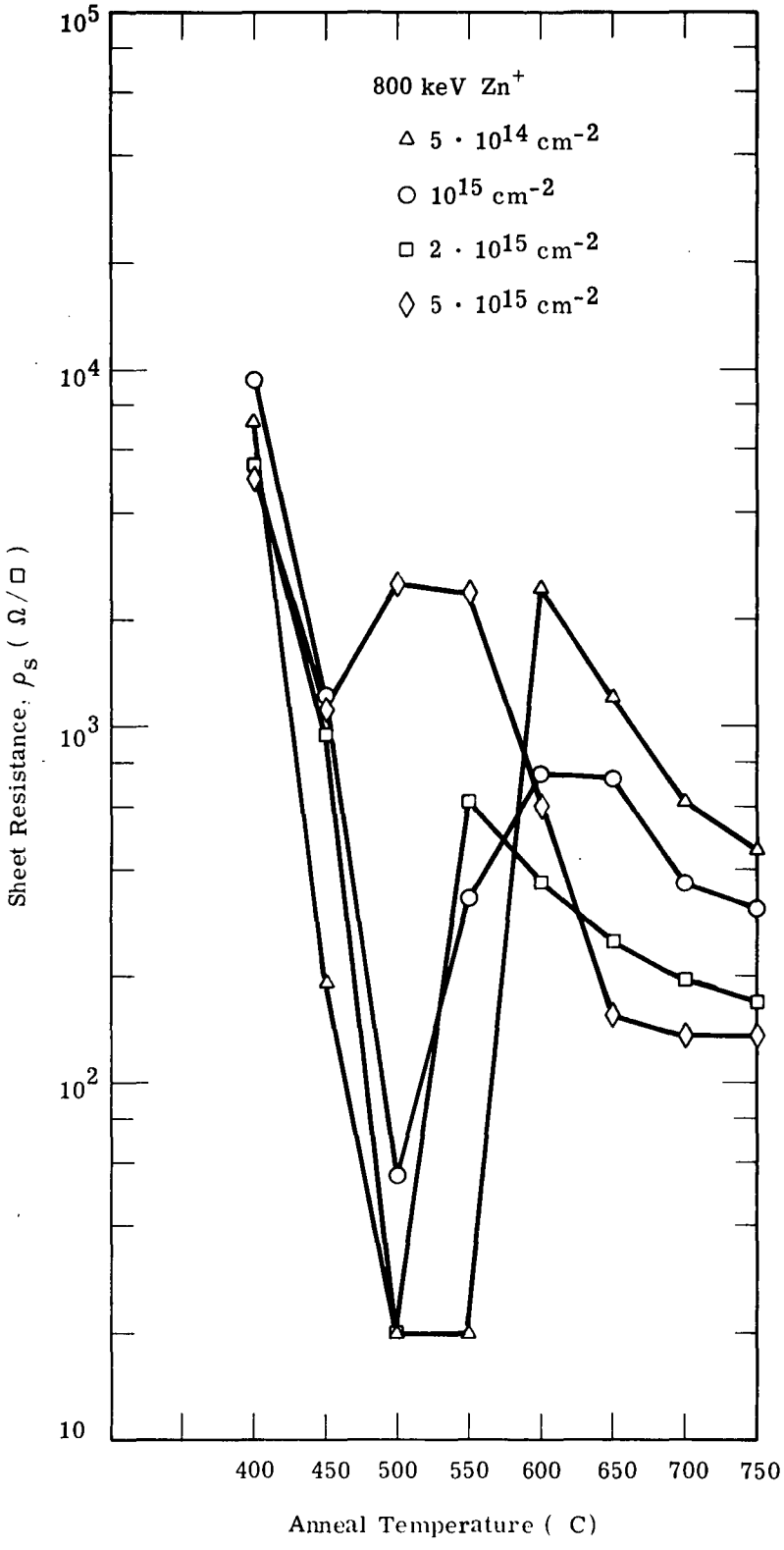

Figure 5. Annealing Characteristics for 800 keV Zinc Implants in GaAs.

1-6364

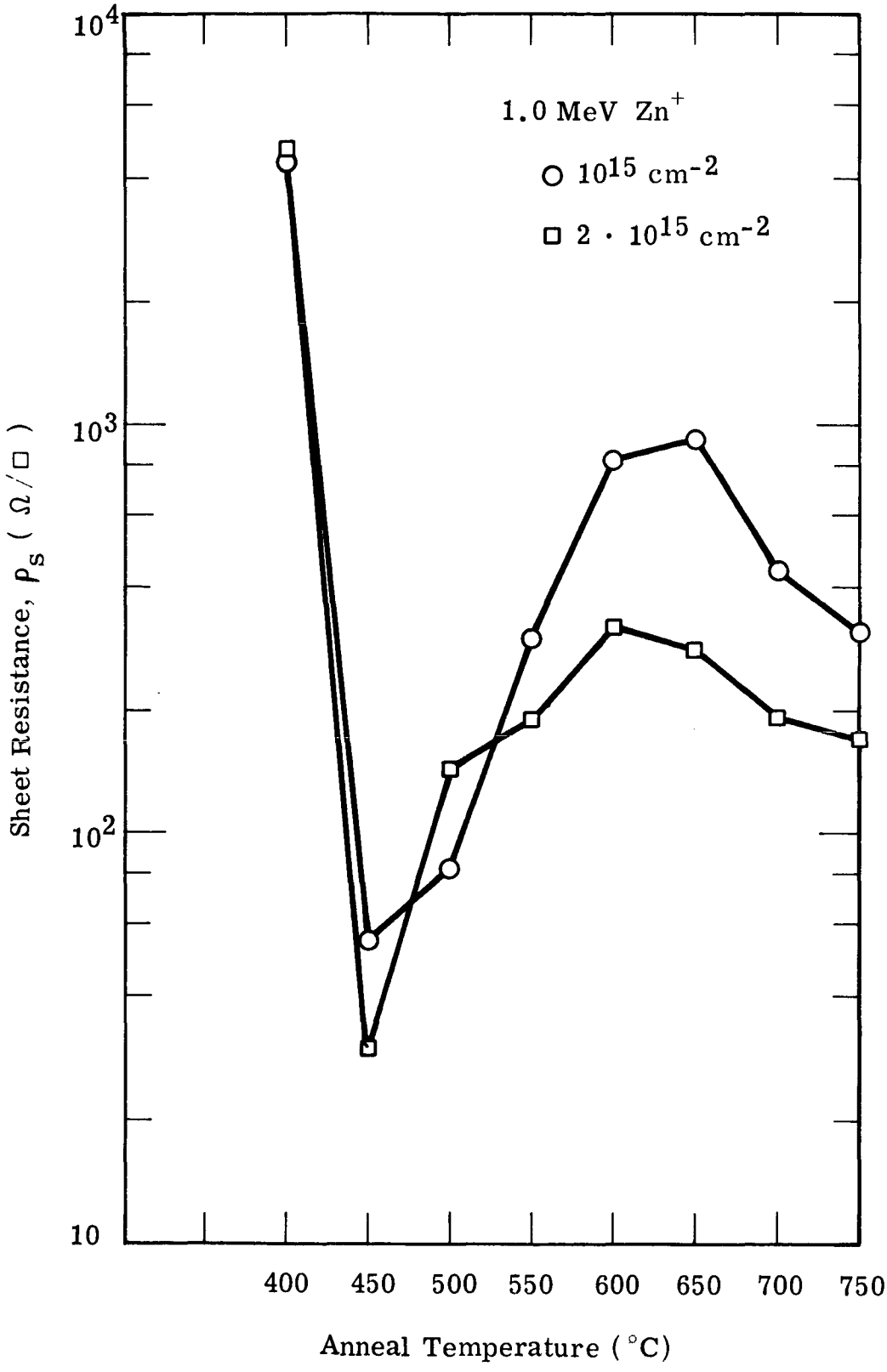

Figure 6. Annealing Characteristics for 1.0 MeV Zinc Implants in GaAs.

1-6365

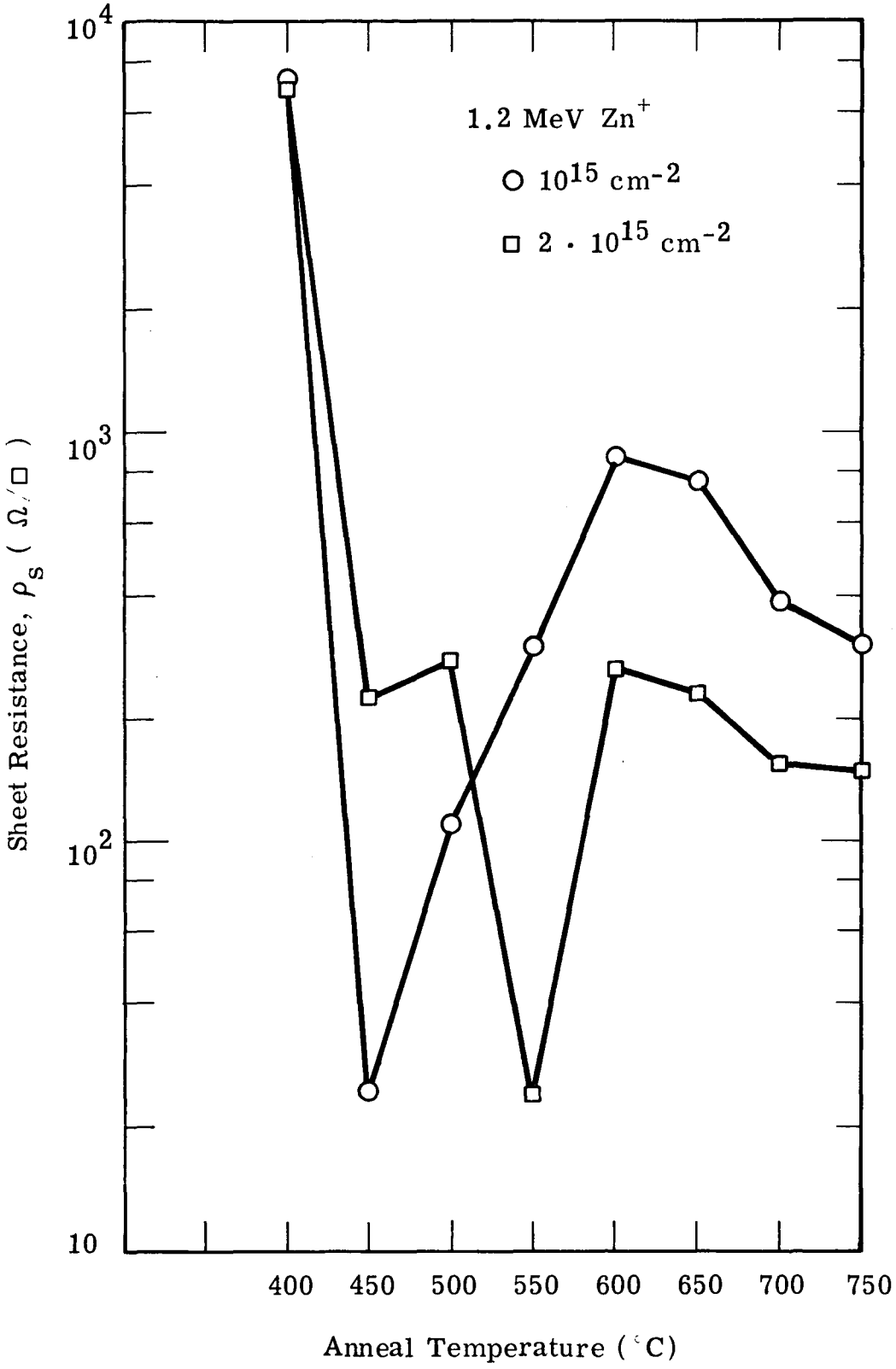

Figure 7. Annealing Characteristics for 1.2 MeV Zinc Implants in GaAs.

1-6366

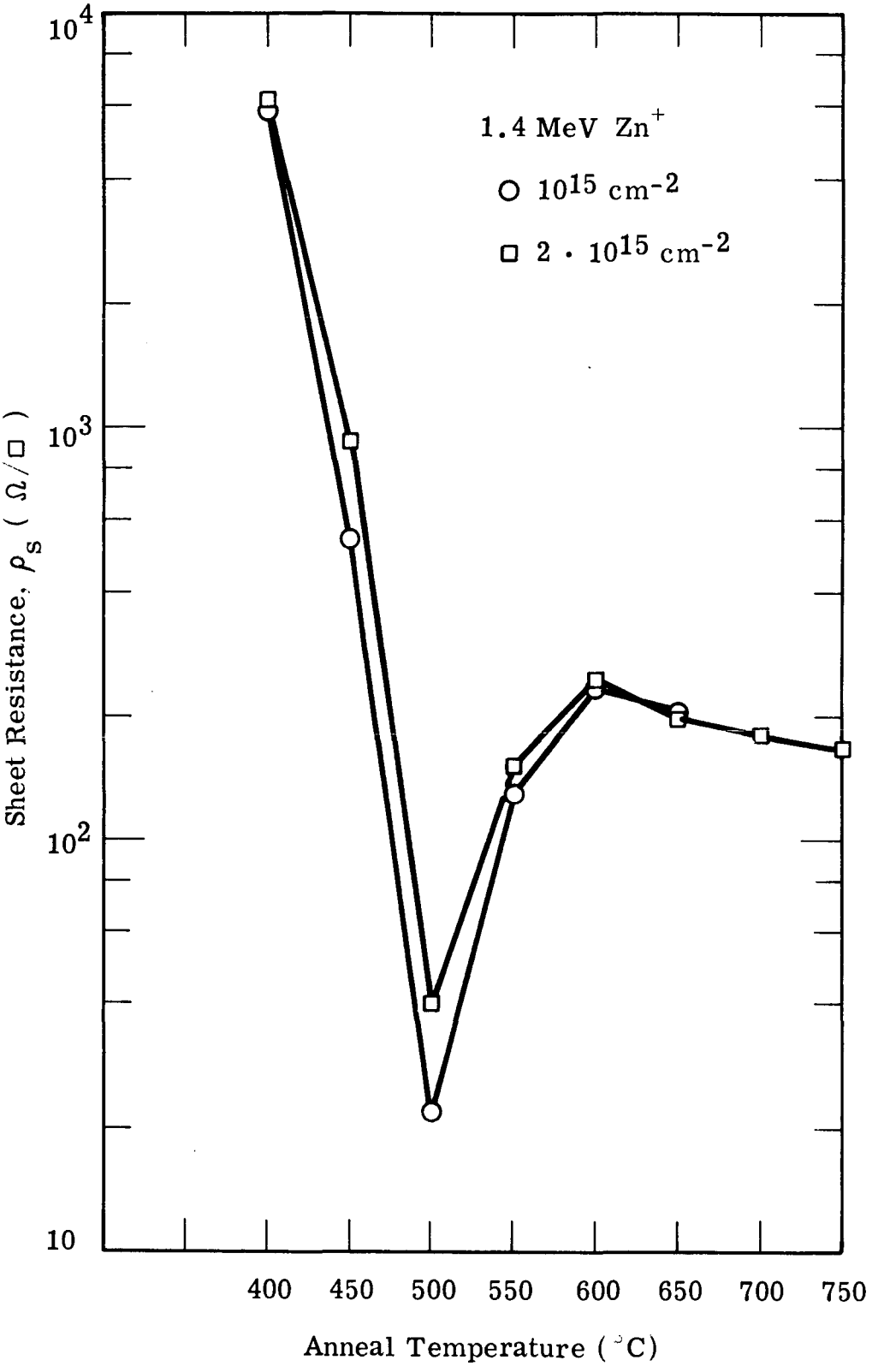

Figure 8. Annealing Characteristics for 1.4 MeV Zinc Implants in GaAs.

1-6368

All samples showed a decrease in sheet resistance for increasing dose. With the exception of the 200 keV samples, the samples showed a factor of ~two decrease in sheet resistance for a corresponding increase in dose up to dose levels of 2×10^{15} cm^{-2}. Above this value saturation effects appear to occur. This is shown in Figure 9 for 600 and 800 keV samples implanted with doses between 5×10^{14} cm^{-2} and 5×10^{15} cm^{-2}. The figure also shows the effect of annealing temperatures of 700 °C and 750 °C for this dose range. It should be pointed out that decreased dopant solubility and lower mobility characteristic of highly doped GaAs would tend to add to the appearance of a saturation effect.

Figures 10 through 12 show sheet resistance versus implant energy for 10^{15} cm^{-2} and 2×10^{15} cm^{-2} dose and annealing temperatures between 650 °C and 750 °C. Variations in sheet resistance between the various implant energies becomes progressively smaller as the anneal temperature increases. At 750 °C essentially a constant value is reached, which is independent of implant energy. Figure 12 shows more clearly the factor of two differences in sheet resistance for the corresponding difference in implanted dose.

2.2.3 Junction Depth Measurements

Another important solar cell parameter in GaAs is junction depth. The analytical results showed a strong dependence of cell output characteristics on junction depth particularly at higher surface layer carrier concentrations. The implantation energy and substrate carrier concentration determine junction depth. This was discussed in some detail in Quarterly Report No. 1 and theoretical curves for projected range, junction depth and implantation profiles were presented (Figures 14 and 15) in that report.

Upon completion of the above anneals, the samples were angle lapped and stained to delineate the junction. The results of these measurements are contained in Table 1. The accuracy of these measurements are approximately 1000 Å. Figure 13 contains photographs of angle sections taken on several representative samples. All values given in the table represent measurements on samples annealed at 750 °C. Comparison with measurements made on samples annealed at lower temperatures (600 °C - 700 °C) show no apparent diffusion taking place. Figure 14 shows measured values plotted against implant energy for 10^{15} cm^{-2} dose. The solid curves represent calculations for projected range (R_p) and junction depths (x_1, x_2, x_3) for the ratios of dopant concentration indicated. Using the computed values for carrier concentration contained in Table 1 and the respective substrate concentration to obtain the dopant ratio, the measured values agree closely with predicted curves.

Table 1. Characteristics of Zinc Implants in n-type GaAs.

Implant Energy E (keV)	Dose N (cm^{-2})	Sheet Resistance ρ_S ($\Omega/\square$)	Junction Depth x_j (μm)	Resistivity $\bar{\rho} = \rho_S x_j$	N_A (cm^{-3})
Background Concentration, $N_B = 2 \times 10^{17}$ cm^{-3}					
200	10^{15}	345	0.12 - 0.15	$4.65 \cdot 10^{-3}$	$2.1 \cdot 10^{19}$
	$2 \cdot 10^{15}$	286	0.12 - 0.15	$3.86 \cdot 10^{-3}$	$2.3 \cdot 10^{19}$
400	10^{15}	195	0.3	$5.7 \cdot 10^{-3}$	$1.5 \cdot 10^{19}$
	$2 \cdot 10^{15}$	Sample Lost in Processing			
600	$5 \cdot 10^{14}$	490	0.38	$1.86 \cdot 10^{-2}$	$2.5 \cdot 10^{18}$
	10^{15}	318	0.38	$1.21 \cdot 10^{-2}$	$5 \cdot 10^{18}$
	$2 \cdot 10^{15}$	177	0.38	$6.72 \cdot 10^{-3}$	$1.2 \cdot 10^{19}$
	$5 \cdot 10^{15}$	145	0.44	$6.38 \cdot 10^{-3}$	$1.3 \cdot 10^{19}$
800	$5 \cdot 10^{14}$	453	0.4	$1.81 \cdot 10^{-2}$	$2.5 \cdot 10^{18}$
	10^{15}	308	0.51	$1.57 \cdot 10^{-2}$	$3 \cdot 10^{18}$
	$2 \cdot 10^{15}$	168	0.51	$8.56 \cdot 10^{-3}$	$9 \cdot 10^{18}$
	$5 \cdot 10^{15}$	136	0.64	$8.7 \cdot 10^{-3}$	$8 \cdot 10^{18}$
1000	10^{15}	313	0.63	$1.97 \cdot 10^{-2}$	$2.1 \cdot 10^{18}$
	$2 \cdot 10^{15}$	172	0.70	$1.2 \cdot 10^{-2}$	$5 \cdot 10^{18}$
1200	10^{15}	304	0.76	$2.31 \cdot 10^{-2}$	$1.8 \cdot 10^{18}$
	$2 \cdot 10^{15}$	150	0.82	$1.23 \cdot 10^{-2}$	$5 \cdot 10^{18}$
1400	10^{15}	-	0.88	Sample Lost in Processing	
	$2 \cdot 10^{15}$	168	0.88	$1.48 \cdot 10^{-2}$	$3 \cdot 10^{18}$
Background Concentration, $N_B = 1 \times 10^{16}$ cm^{-3}					
600	10^{15}	170	0.5	$8.5 \cdot 10^{-3}$	10^{19}
	10^{15}	160	0.5	$8.0 \cdot 10^{-3}$	10^{19}
800	10^{15}	81	0.64	$5.2 \cdot 10^{-3}$	$1.7 \cdot 10^{19}$

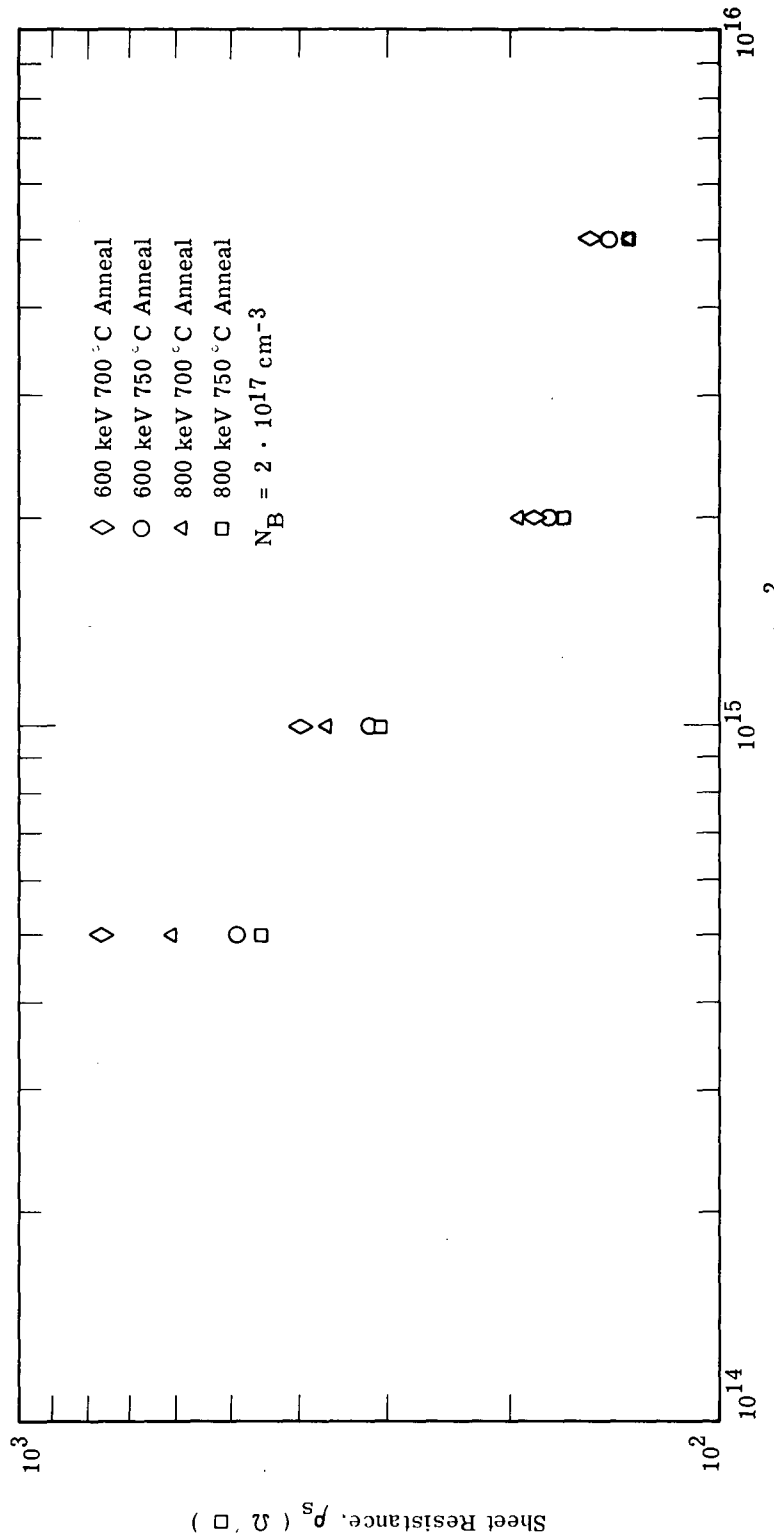

Figure 9. Sheet Resistance versus Implanted Dose for 600 and 800 keV Zinc in GaAs at Two Anneal Temperatures.

1-6368

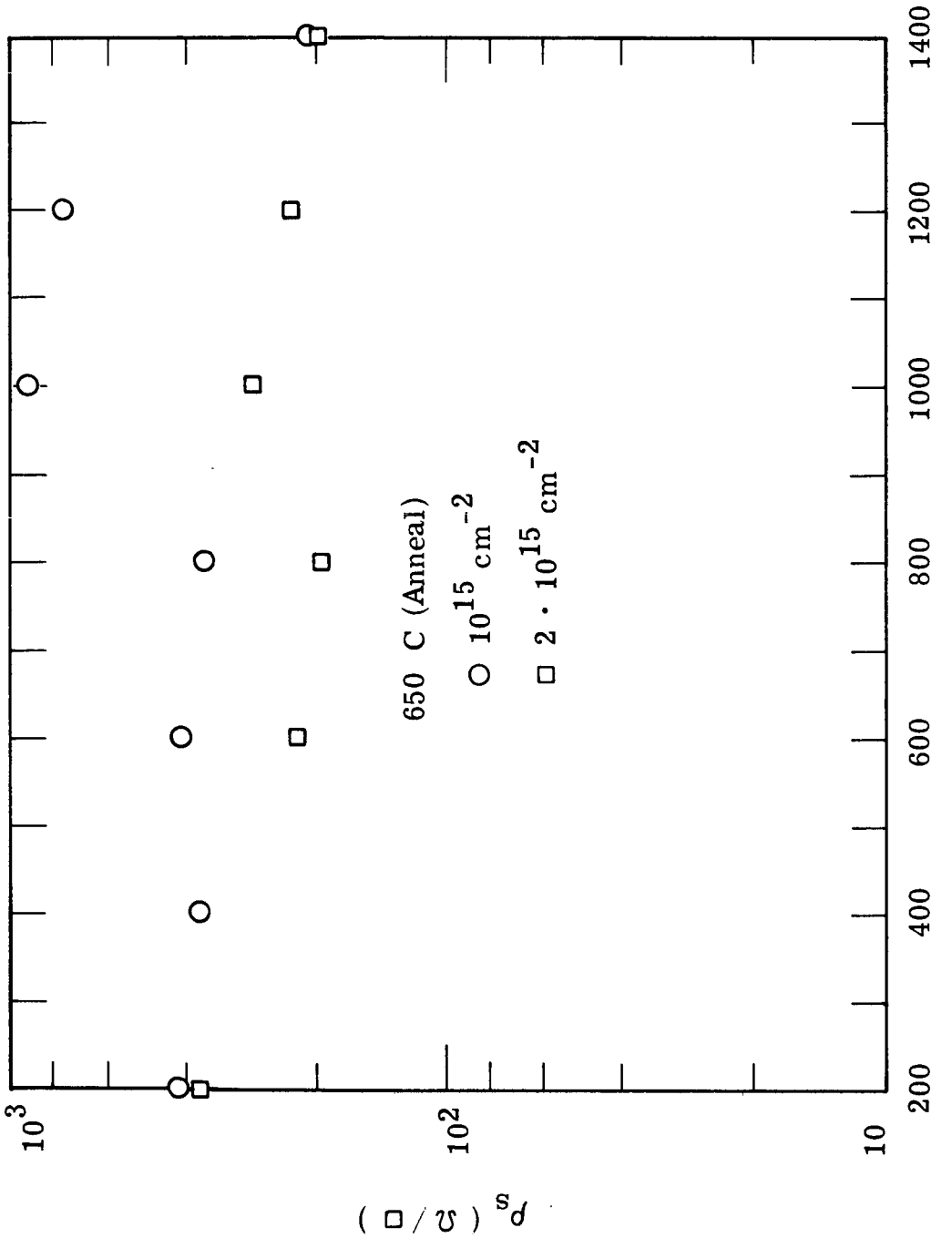

Figure 10. Sheet Resistance versus Implant Energy for 10^{15} cm^{-2} $2 \cdot 1015$ cm^{-2} Dose Annealed at 650 °C.

1-6369

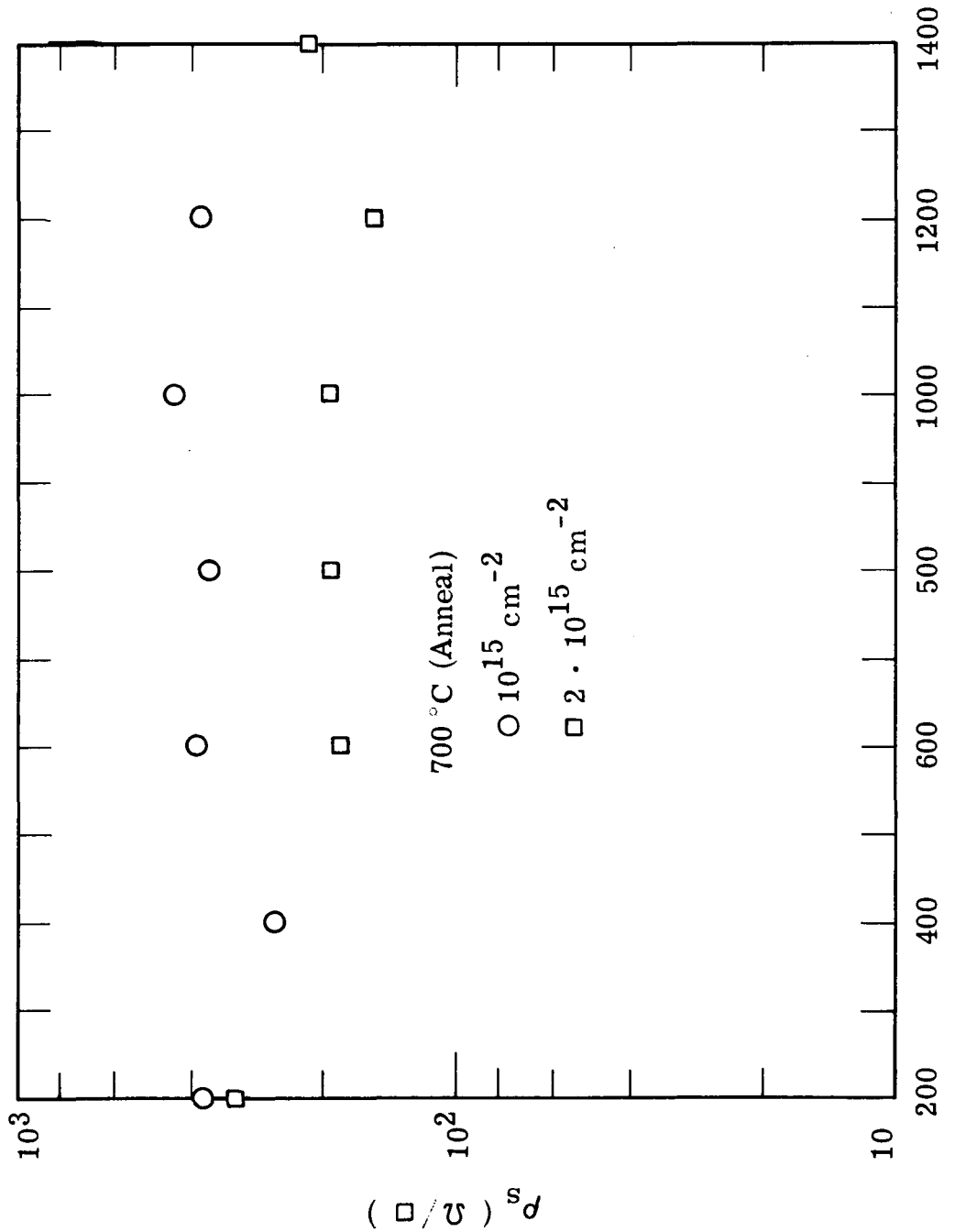

Figure 11. Sheet Resistance versus Implant Energy for 10^{15} cm^{-2} and 2 · 1015 cm^{-2} Dose Annealed at 700 °C.

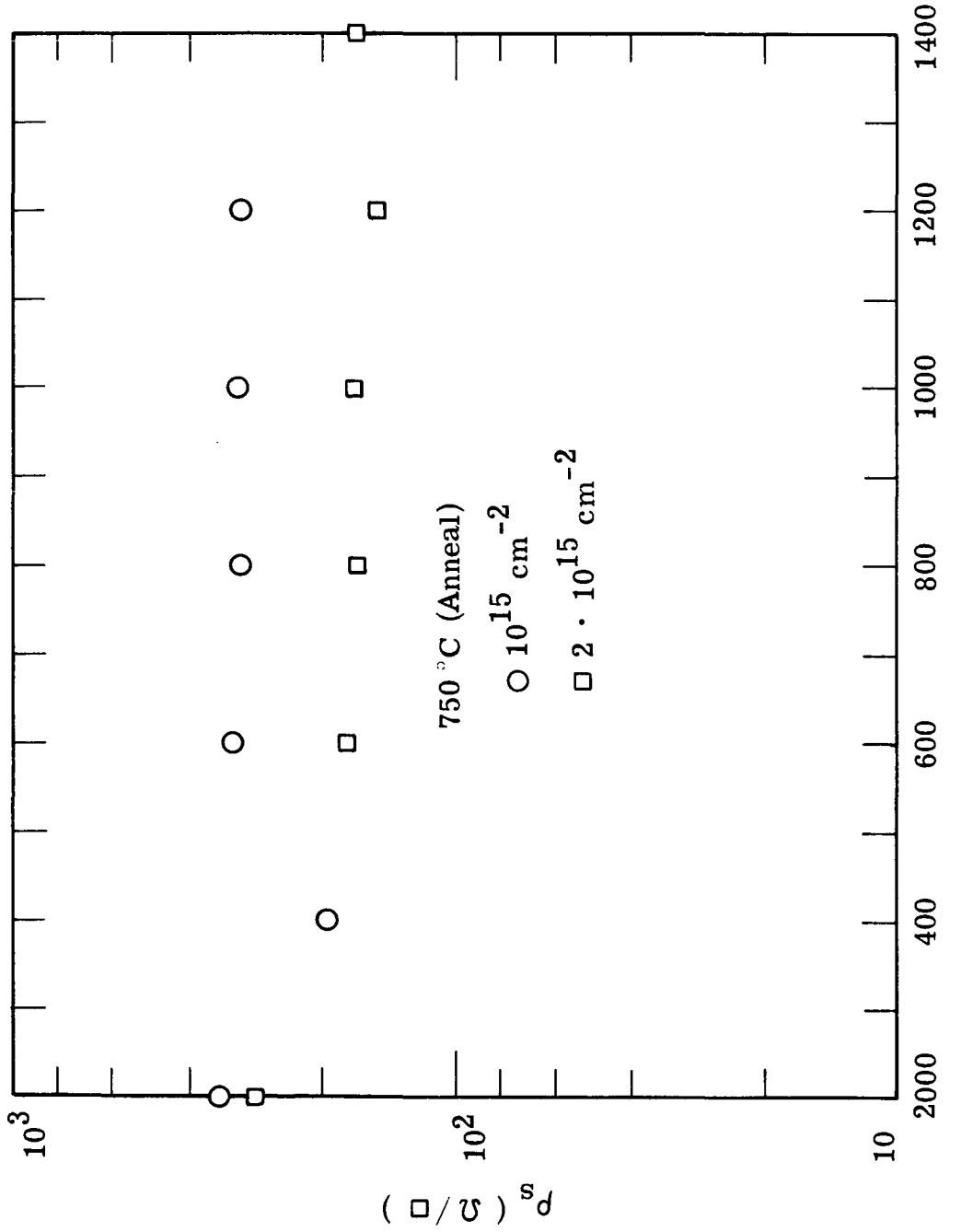

Figure 12. Sheet Resistance versus Implant Energy for 10^{15} cm^{-2} and $2 \cdot 10^{15}$ cm^{-2} Dose Annealed at 750 °C.

1-6371

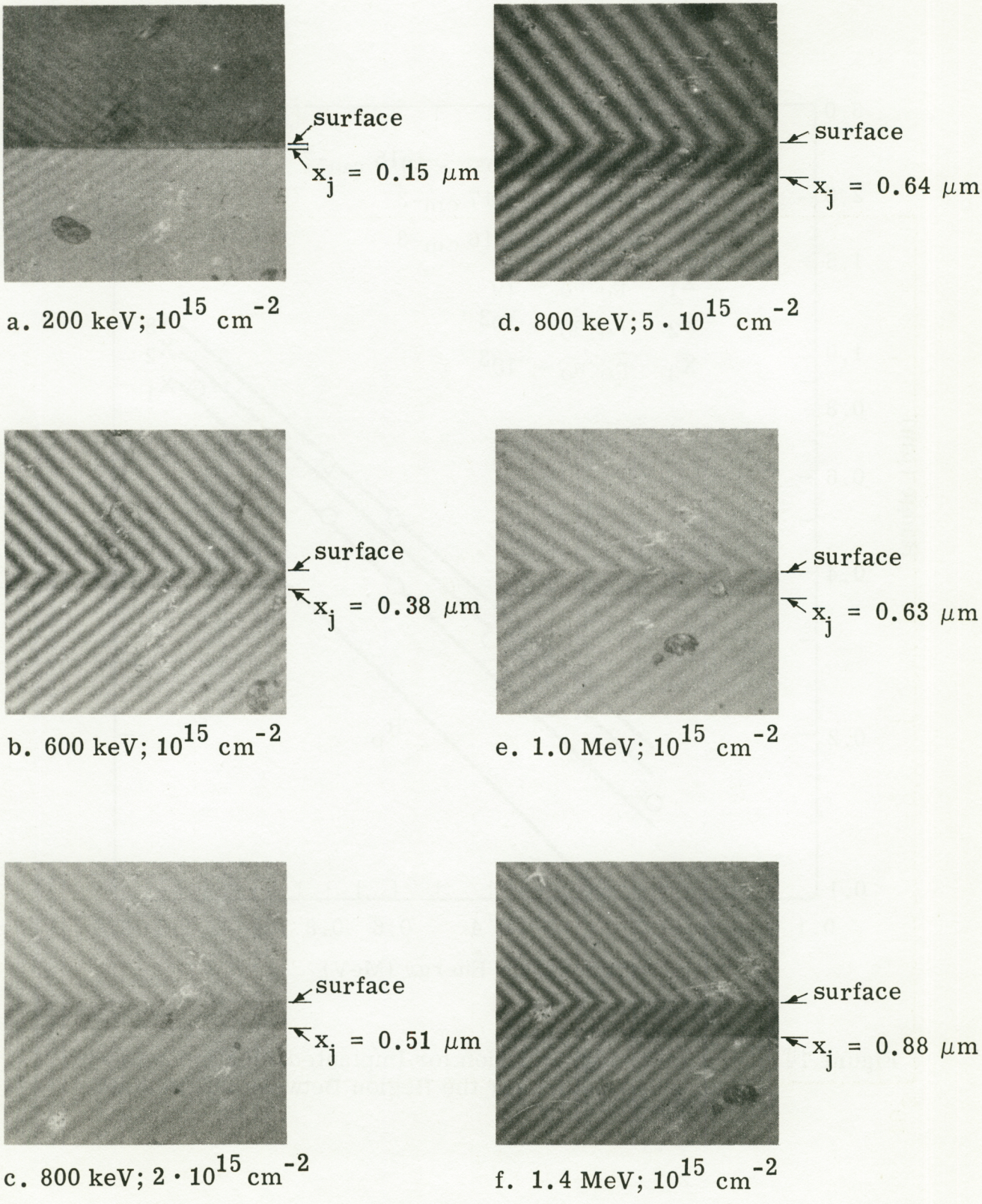

Figure 13. Photographs of Junction Delineation in GaAs for Several Implant Conditions.

2-1614

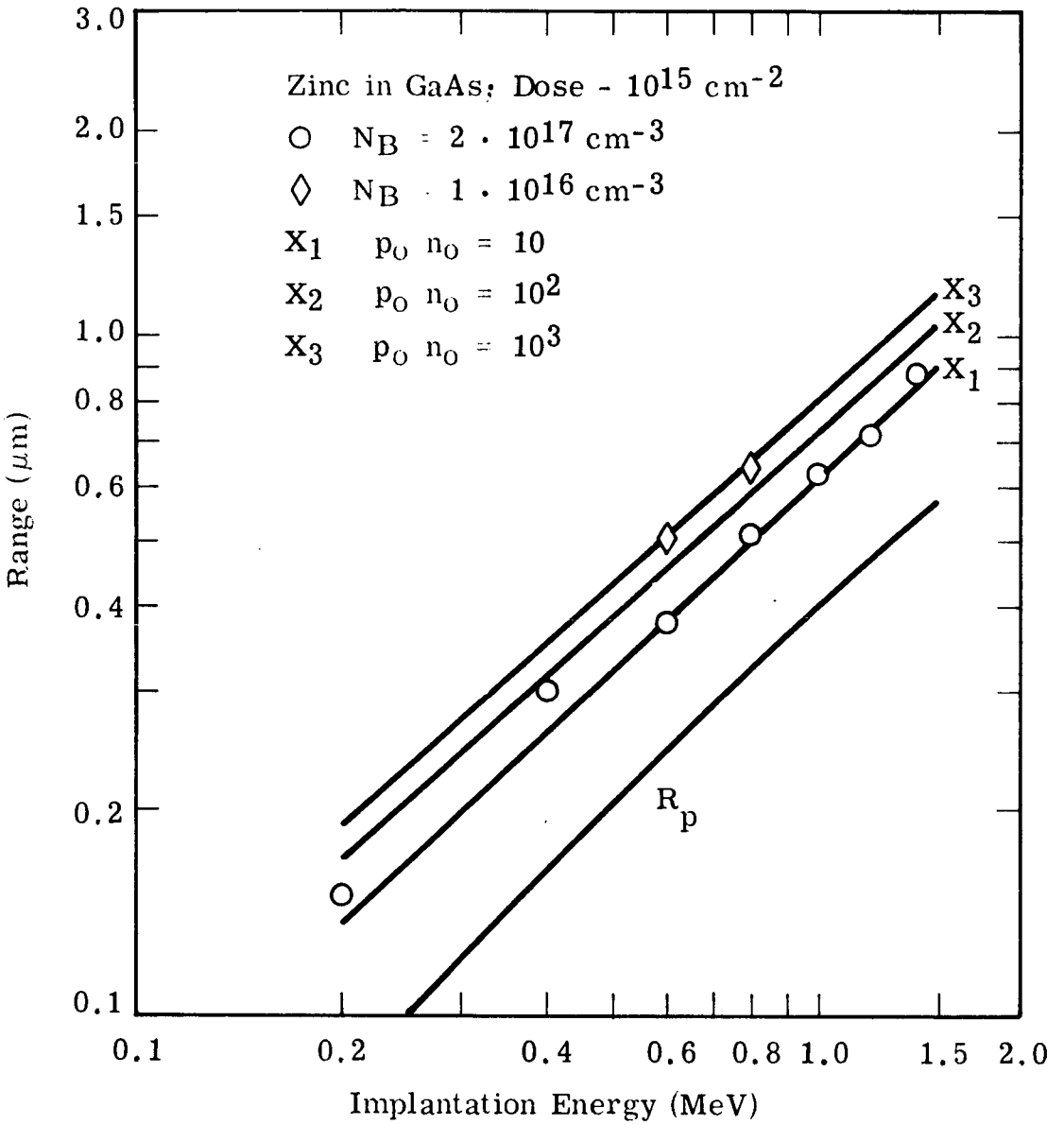

Figure 14. Range-Energy Relation for Implanted Zinc in GaAs with Measured Values for the Region Between 200 keV and 1.4 MeV.

1-6373

2.2.4 Junction Characterization

Preliminary work on junction characterization and electrical contacting of the annealed samples was started during this report period. The contact alloy, In-Ag (25:75 wt. %) was used to contact both substrate and implanted regions. The contacting procedure consisted of sequential evaporation of In followed by the Ag on heated substrates (~300 °C). After evaporation contacts to the substrate were formed at ~500 °C for 10 minutes; contacts to the surface layer were not fired after the evaporation. Figure 15 shows V-I characteristics of contacts deposited on the 800 keV, $2 \cdot 10^{15}$ Zn/cm^2 sample. Approximate specific contact resistance values are 2×10^{-2} Ω cm^2 and 9×10^{-4} Ω cm^2 for the surface layer and substrate contacts respectively. Improvement will be required in lowering these values for both regions in a finished solar cell; however, they are adequate for the present in evaluating junction characteristics.

Figure 16 shows current-voltage characteristics for mesa diodes formed on the above sample. Both the dark and illuminated characteristics are shown. Work is underway to analyze both I-V and C-V behavior for all of the above annealed samples.

2.2.5 Summary

Results of the annealing study show that temperatures near 750 °C are required to produce carrier concentrations greater than 10^{19} cm^{-3} by zinc implantation. Sheet resistances between 100 and 200 Ω/□ can be realized by implanting at 400 keV and higher with dose levels above 10^{15} cm^{-2}. Some dependence on substrate carrier concentration was observed in the values obtained. These results together with junction depth measurements indicate that effort should be concentrated in studying implant energies of 600 - 800 keV and dose levels between 10^{15} cm^{-2} and 5×10^{15} cm^{-2} to optimize the annealing cycle. These values are approximately the ones required to produce the cell structure based on the analytical results.

Results of junction depth measurements agree closely with theoretically predicted values. The data obtained will be used in specifying the cell fabrication process for both cell polarities since the predicted range of selenium in GaAs (N/P cell) closely approximates the values for zinc. Experimental confirmation of this will be made in the planned study on selenium implants.

The results show that additional effort on zinc implants is required in the areas of annealing, contact metallurgy, junction characterization and study of implanted profiles.

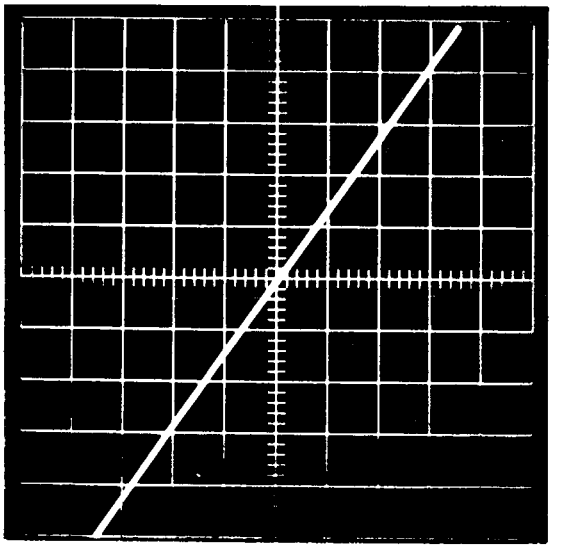

Surface Layer Electrical Contacts (I = 2 mA/div./V = 200 mV/div.)

($R_c \approx 2 \cdot 10^{-2}\ \Omega\,cm^2$)

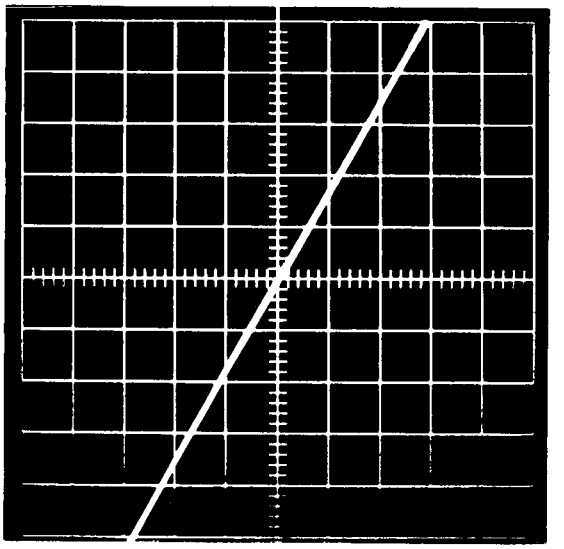

Substrate Electrical Contacts (I = 20 mA/div./V = 20 mV/div.)

($R_c \approx 9 \cdot 10^{-4}\ \Omega\,cm^2$)

Figure 15. V-I Characteristics for In:Ag Electrical Contacts on GaAs.

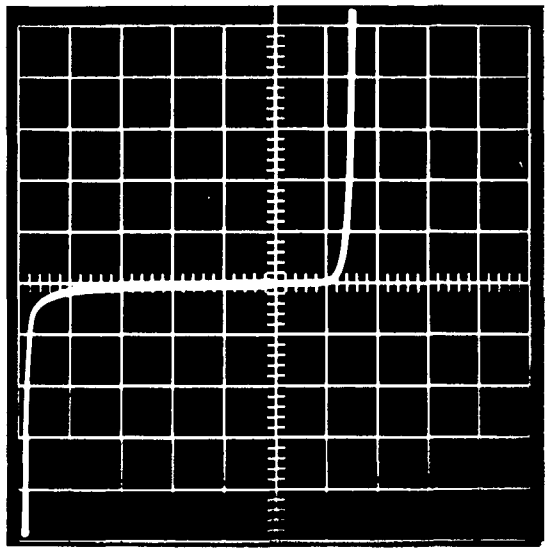

←V = 2 V/div. V = 0.5 V/div.→
I = 0.1 mA/div.

I-V Diode Characteristic

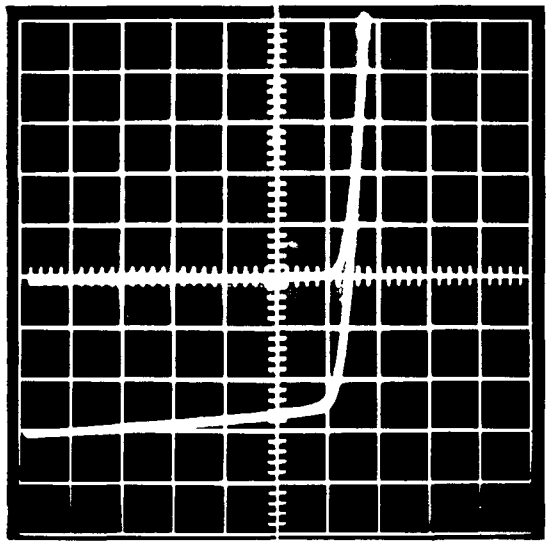

V = 0.5 V/div.
I = 0.1 mA/div.

Illuminated I-V Characteristic

Figure 16. V-I Characteristics for a Zinc Implanted Diode in GaAs (800 keV, 2×10^{15} cm^{-2}, $N_B = 2 \times 10^{17}$ cm^{-3}).

2-1616

SECTION 3

PLANNED WORK

The next report period will be concerned with junction characterization of the zinc implants, improvement in contact metallurgy and additional zinc implants for refinement of the anneal cycle. An attempt will be made to determine the implanted zinc profile. Formation of n-type surface layers by implantation of selenium and characterization similar to the zinc studies will be initiated. We expect to have sufficient data on the most significant solar cell process steps at the end of this period to begin Phase II - fabrication of the first lot of experimental cells.